RESEARCH PAPER

Rubiarbonone C inhibits platelet-derived growth factor-induced proliferation and migration of vascular smooth muscle cells through the focal adhesion kinase, MAPK and STAT3 Tyr705 signalling pathways

Correspondence Chang-Seon Myung, Department of Pharmacology, Chungnam National University College of Pharmacy, 99 Daehak-ro (St.), Yuseong-gu, Daejeon 34134, Korea, and MinKyun Na, College of Pharmacy, Chungnam National University, 99 Daehak-ro (St,), Yuseong-gu, Daejeon 34134, Korea. E-mail: cm8r@cnu.ac.kr; mkna@cnu.ac.kr

Hyun-Soo Park[1],*, Khong Trong Quan[2,3],*, Joo-Hui Han[1], Sang-Hyuk Jung[1], Do-Hyung Lee[1], Eunji Jo[1], Tae-Wan Lim[1], Kyung-Sun Heo[1], MinKyun Na[2,4] and Chang-Seon Myung[1,4] (iD)

[1]Department of Pharmacology, Chungnam National University College of Pharmacy, Daejeon, Korea, [2]Department of Pharmacognosy, Chungnam National University College of Pharmacy, Daejeon, Korea, [3]Department of Pharmaceutical Analysis and Standardization, National Institute of Medicinal Materials, Hanoi, Vietnam, and [4]Institute of Drug Research and Development, Chungnam National University, Daejeon, Korea

*These two authors contributed equally to this work.

BACKGROUND AND PURPOSE
The proliferation and migration of vascular smooth muscle cells (VSMCs) induced by platelet-derived growth factor (PDGF) are important steps in cardiovascular diseases, including neointimal lesion formation, myocardial infarction and atherosclerosis. Here, we evaluated the rubiarbonone C-mediated signalling pathways that regulate PDGF-induced VSMC proliferation and migration.

EXPERIMENTAL APPROACH
Cell proliferation and migration were measured in cells treated with rubiarbonone C followed by PDGF BB using the MTT assay, [^{3}H]-thymidine incorporation, flow cytometry and wound-healing migration assay, MMP gelatin zymography, a fluorescence assay for F-actin. Western blotting of molecules including MAPK, focal adhesion kinase (FAK) and STAT3 and an immunofluorescence assay using anti-PCNA and -STAT3 antibodies were performed to evaluate rubiarbonone C signalling pathway(s). The medial thickness of the carotid artery was evaluated using a mouse carotid ligation model.

KEY RESULTS
Rubiarbonone C inhibited PDGF-induced VSMC proliferation and migration and diminished the ligation-induced increase in medial thickness of the carotid artery. In PDGF-stimulated VSMCs rubiarbonone C decreased the following: (i) levels of cyclin-dependent kinases, cyclins, PCNA and hyperphosphorylated retinoblastoma protein; (ii) levels and activity of MMP2 and MMP9; (iii) activation of MAPK; (iv) F-actin reorganization, by reducing FAK activation; (v) activation of STAT3.

CONCLUSIONS AND IMPLICATIONS
These findings suggest that rubiarbonone C inhibits the proliferation and migration of VSMCs by inhibiting the FAK, MAPK and STAT3 signalling pathways. Therefore, rubiarbonone C could be a good candidate for the treatment of cardiovascular disease.

Abbreviations
CDK, cyclin-dependent kinases; FAK, focal adhesion kinase; LCA, left carotid artery; PDGF, platelet-derived growth factor; pRb, retinoblastoma protein; STAT3, signal transducer and activator of transcription 3; VSMC, vascular smooth muscle cell

Introduction

The excessive proliferation and migration of abnormal vascular smooth muscle cells (VSMCs) are major causes of the development and progression of cardiovascular diseases, such as restenosis and atherosclerosis (Chistiakov *et al.,* 2015). Platelet-derived growth factor (PDGF) is an important factor regulating cardiovascular remodelling (Yin and Agrawal, 2014); PDGF consists of five isoforms: AA, AB, BB, CC and DD (Fredriksson *et al.,* 2004). Among them, the transcript levels of **PDGF BB** are uniquely increased in human atherosclerotic plaques versus normal arteries (Cagnin *et al.,* 2009). Additionally, it has been shown that PDGF BB, as a potent mitogen, induces VSMC migration and intimal hyperplasia in rat, mouse and porcine arteries in carotid injury models *in vivo* (Jun *et al.,* 2016).

Progression of the cell cycle is an important aspect of cell proliferation. The cell cycle consists of four phases: G_0/G_1, S, G_2 and M. VSMCs in normal arteries are usually quiescent and exist in the G_0 phase. When VSMCs are stimulated by various vascular pathologies, such as injury and the resulting growth factors, the level of the cyclin and cyclin-dependent kinase (CDK) complex is elevated, with sequential hyperphosphorylation of retinoblastoma protein (pRb) (Lee *et al.,* 2011b). Then, DNA is synthesized in the S phase, leading to VSMC proliferation (Bicknell *et al.,* 2003).

The levels and activity of **MMP2** and **MMP9** are important in VSMC migration (Kim and Ko, 2014). VSMCs undergo a rapid and reversible change from a quiescent contractile phenotype to a proliferative synthetic phenotype, induced by increased degradation of extracellular matrix proteins, such as gelatin and collagen (Chaabane *et al.,* 2013). Such decomposition of the extracellular matrix facilitates the induction of VSMC migration (Li *et al.,* 2015). Phosphorylation of focal adhesion kinase (**FAK**) has a significant effect on VSMC migration by affecting cytoskeletal remodelling. Furthermore, the reorganization of F-actin to facilitate cell movement is controlled by FAK activation (da Silva *et al.,* 2015).

PDGF receptor-β (PDGFR-β)-mediated signalling pathways, including **MAPK**s (Lee *et al.,* 2011a), **PKB (Akt)**, PKC (Chandra and Angle, 2006) and FAK (Chan *et al.,* 2014), have been suggested to affect cell proliferation and migration. Furthermore, accumulating evidence supports an important role for the activation of signal transducer and activator 3 (STAT3) in PDGF BB-induced VSMC proliferation and migration (Heiss *et al.,* 2016). Moreover, STAT3 down-regulation contributes to the reduced activation of cyclin D, intracellular adhesion molecule-1, MMP9 and pRb (Park *et al.,* 2015), which are key regulators of abnormal vascular remodelling. However, how STAT3 activation mediates both PDGF BB-induced cell proliferation and migration is not well understood. In particular, whether PDGF BB-induced PDGFR-β-mediated signalling pathways influence STAT3 activation in regulating cell proliferation and migration processes remains largely unknown.

Rubiarbonone C is one of the major triterpenoids of the *Rubia philippinensis* Elmer (family Rubiaceae) plant (Elmer, 1934). *R. philippinensis* is a perennial herb and a well-known traditional Korean medicine, listed in the Korean Pharmacopoeia (Chen *et al.,* 1999). *R. philippinensis* has been reported to have beneficial anticancer activity (Lajko *et al.,* 2015) and a protective effect against kidney oxidative damage (Lodi *et al.,* 2011). Phytochemical studies have shown the major constituents of this plant, which include *Rubiaceae*-type bicyclic hexapeptides (Lee *et al.,* 2008), anthraquinones (Fan *et al.,* 2011) and triterpenoids (Liou and Wu, 2002). Gao *et al.* (2014) examined the antihyperlipidaemic effects of extracts and compounds of the *Rubia yunnanensis* roots and found that rubiarbonone C is one of the major compounds responsible for this activity. The triterpenoids are known to have important antioxidant and anti-inflammatory properties in various pathologies related to fibrosis and cardiac remodelling (Kuok *et al.,* 2013; Garcia-Rivas *et al.,* 2015; Muhammad *et al.,* 2015; Amoussa *et al.,* 2016). However, the effects of rubiarbonone C on abnormal vascular remodelling remain unclear. Thus, we investigated the inhibitory effects of rubiarbonone C on PDGF BB-mediated signalling pathways in VSMC proliferation and migration, which are key steps contributing to abnormal vascular remodelling.

Methods

Animals

Animal studies are reported in compliance with the ARRIVE guidelines (Kilkenny *et al.,* 2010; McGrath and Lilley, 2015). All animal experiments including the isolation of rat VSMCs from the aorta and mouse carotid ligation were performed with the approval of the Chungnam National University Animal Care and Use Committee (approval protocol number CNU-00826).

Isolation of VSMCs

The male Sprague Dawley rats (average weight 300 g and 7 weeks-old) were maintained under pathogen-free conditions at the College of Pharmacy at the Chungnam National University. These rats were purchased from Samtako (Osan, Gyeonggi-do, Korea). The rats were killed with an overdose of pentobarbital. Rat aortic VSMCs were isolated by enzymatic dispersion as described previously (Sachinidis *et al.,* 1995).

Mouse carotid ligation model

Animal experiments using mouse carotid ligation model were carried out using male C57BL/6 mice (average weight 23 g and 6 weeks-old) in accordance with the ARRIVE guidelines (Kilkenny *et al.,* 2010; McGrath and Lilley, 2015). Mice were purchased from Samtako (Osan, Gyeonggi-do, Korea). The animals were randomly assigned to the different treatment groups. The animals were treated with an i.p. injection of 0.3 or 1.2 mg·kg⁻¹ rubiarbonone C (*n* = 8 per group). Eight vehicle-treated animals (150 μL of 5% DMSO i.p.) served as controls. Subsequently, the left carotid artery (LCA) was ligated, as previously described (McPherson *et al.,* 2001). Briefly, the mice were anaesthetized by an i.p. injection of 50 mg·kg⁻¹ pentobarbital, and this state was maintained by inhalation of 1–2.5% isoflurane with oxygen, the LCA was exposed and completely ligated. The depth of anesthesia is confirmed by toe pinch. The operation was performed, when there was no reaction (leg or body movement) after

anesthesia. The mice were then allowed to recover while being kept warm on a heated pad and pain-free by treatment with 1% ketoprofen (0.2 mL·kg^{-1} s.c.). After 3 days of ligation, the mice were killed by an overdose of pentobarbital, and carotid arteries and other organs (liver, lung, heart, spleen and kidney) were harvested. The organs were fixed and embedded in paraffin for histological analysis.

Dosing protocol

One day before LCA ligation, test groups were treated with 10 or 40 μM rubiarbonone C (injected rubiarbonone C per total blood volume, i.p.). According to the Guidelines of the National Centre for the Replacement Refinement and Reduction of Animals in Research, the mouse has around 58.5 mL of blood kg^{-1} of bodyweight. The correct doses of rubiarbonone C, 10 μM (0.3 mg·kg^{-1}) or 40 μM (1.2 mg·kg^{-1}), were injected three times to animals in the test groups on day 1 before ligation and days 1 and 2 after ligation.

Histological analysis

Serial sections (5 μm) at 150 μm intervals were taken from the LCA, right carotid artery and the 5 μm sections of liver, lung, heart, spleen and kidney were prepared. These were then stained using haematoxylin and eosin (Heo et al., 2014a,b). To determine the medial thickness, the distance between the internal elastic lamina and external elastic lamina was measured by Image j software.

Cell culture

Rat aortic VSMCs were cultured in DMEM, supplemented with 10% (vv^{-1}) FBS, 100 IU·mL^{-1} penicillin, 100 μg·mL^{-1} streptomycin, 4.5 g·L^{-1} D-glucose, 110 mg·L^{-1} sodium pyruvate and 2 mM L-glutamine at 37°C in a humidified atmosphere of 95% air and 5% CO$_2$. VSMCs were used at passages 4–9.

Cell proliferation and viability assays

PDGF BB-induced VSMC proliferation and cell viability were determined using the 3-(4, 5-dimethylthiazol-2-yl)-2, 5-diphenyltetrazolium bromide (MTT) assay, as described previously (Hu et al., 2014). Briefly, VSMCs were seeded in a 96-well plate at 3.0 × 10^4 cells·mL^{-1} and cultured in DMEM containing 10% FBS at 37°C for 24 h. After incubation in serum-free DMEM for 24 h, the cells were pretreated with various concentrations (5, 10 and 20 μM) of rubiarbonone C for 24 h, followed by treatment with 25 ng·mL^{-1} PDGF BB for another 24 h. For the viability assay, serum-starved VSMCs were treated with 5, 10 or 20 μM rubiarbonone C or 100 μg·mL^{-1} digitonin (cytotoxic control) for 48 h. At the end of the stimulation, the medium was removed, and 200 μL 5 mg·mL^{-1} MTT solution was added to each well for 4 h. After the MTT solution was replaced with 200 μL DMSO, the absorbance was measured at 565 nm using a microplate reader (Infinite M200 PRO, Tecan Group Ltd., Zürich, Switzerland).

DNA synthesis assay

A [^{3}H]-thymidine incorporation assay was used to measure DNA synthesis, as described previously (Kim et al., 2005). Serum-starved VSMCs were treated with various concentrations of rubiarbonone C for 24 h, followed by treatment with 25 ng·mL^{-1} PDGF BB for another 24 h. Then, 2 μCi·mL^{-1} [^{3}H]-thymidine was added to the culture medium and incubated for 4 h. The reaction was stopped by washing with cold PBS containing 10% trichloroacetic acid and ethanol/ether (1:1, vv^{-1}). After the cells were dissolved in cold 0.5 N NaOH for 1 h, the acid-insoluble [^{3}H]-thymidine was collected, mixed with 3 mL scintillation cocktail (Ultimagold; Packard Bioscience, Meriden, CT, USA) and quantified using a liquid scintillation counter (LS3801; Beckman, Düsseldorf, Germany).

Cell cycle progression analysis

Cell cycle progression was determined as described previously (Lee et al., 2011b). Serum-starved VSMCs were stimulated with 25 ng·mL^{-1} PDGF BB for 24 h at 37°C. Then, cells were trypsinized and centrifuged (300 × g, 10 min). The VSMCs were then washed with 1 mL PBS and fixed in 70% ethanol for 24 h at 4°C. After being fixed, the cells were centrifuged (300 × g, 5 min), and the VSMCs were stained with 500 μL propidium iodide (PI) solution (50 μg·mL^{-1} in sample buffer containing 100 μg·mL^{-1} RNase A) at 4°C for 30 min. The fluorescence intensity of the incorporated PI, which reflects the individual nuclear DNA content, was measured, using a flow cytometer (FACSCalibur; Becton Dickinson Co., Fullerton, CA, USA). The proportion of cells in the G$_0$/G$_1$, S and G$_2$/M phases of the cell cycle were analysed using the ModFit LT software (Verity Software House, Topsham, ME, USA).

Cell migration assay

A scratch wound-healing migration assay was performed. When the VSMCs reached 90–100% confluence in culture plate wells, cells were subjected to serum-free medium for 24 h. After serum starvation, two lines within the VSMCs were scraped using a sterile plastic pipette tip in each cultured well. The cells were washed twice in warm serum-free medium to remove cellular debris and treated with various concentrations of rubiarbonone C for 2 h, followed by 25 ng·mL^{-1} PDGF BB treatment. After 0 and 48 h, the cells were fixed with 100% cold methanol for 10 min and then stained with 0.5% crystal violet in 25% methanol for 10 min. Images were acquired using a microscope (Nikon Eclipse Ti; Nikon Instruments Inc., Melville, NY, USA), and cell migration was determined by the percentage of the wound closure area in five independent experiments using the Image J software.

MMP gelatin zymography

Gelatin zymography was performed as described previously (Kupai et al., 2010). Briefly, serum-starved VSMCs were pretreated with various concentrations of rubiarbonone C for 2 h, and the cells were stimulated with 25 ng·mL^{-1} PDGF BB for 48 h. After 48 h, the conditioned medium was collected and clarified by centrifugation (8000 × g, 10 min and 4°C). The medium was mixed with non-reducing SDS sample buffer and electrophoresed on a 7.5% SDS-PAGE gel containing 0.1% gelatin. Separated gels were renatured by washing in 2.5% Triton X-100 solution for 1 h to remove SDS in the gel and then incubated in 50 mM Tris–HCl (pH 8.0), 10 mM CaCl$_2$ and 150 μM NaCl at 37°C for 24 h, followed by staining with 0.05% Coomassie brilliant blue R-250 for 1 h. The stained gel was destained in 4% methanol using 8% acetic acid. The activity of MMPs was detected as a clear band on

the blue background of the gel. MMP activity was normalized relative to the total protein concentration in the cell lysate (Kang *et al.,* 2016). The densities of the clear bands were determined using Quantity One software (Bio-Rad, Hercules, CA, USA).

Western blot analysis

Western blotting was performed as described previously (Han *et al.,* 2015). Cell lysates were prepared using RIPA (150 mM sodium chloride, 1% Triton X-100, 1% sodium deoxycholate, 0.1% SDS, 50 mM Tris–HCl, pH 7.5 and 2 mM EDTA) containing proteinase inhibitors. Proteins were subjected to SDS-PAGE and transferred to a PVDF membrane (ATTO Corporation, Tokyo, Japan). After being blocked, the membranes were incubated with primary antibodies to determine the levels of PDGFR-β, **ERK1/2**, **phosphoinositide phospholipase γ-1 (PLCγ1)**, **p38**, **JNK**, **proto-oncogene tyrosine-protein kinase src (Src)**, STAT3, PKC, Akt, myristoylated alanine-rich C-kinase substrate (MARCKS), FAK, MMP2/9, pRb, cyclin D1/E, CDK2/4 and PCNA and the cleavage of PARP and **caspase 3**. The membrane was washed

and incubated with a corresponding horseradish peroxidase-conjugated secondary antibody, and signals were detected using an enhanced chemiluminescence (ECL) Western blotting detection system. The activated proteins were normalized against total protein or β-actin levels. Band intensities were quantified using Quantity One software (Bio-Rad).

Immunofluorescence staining analysis

VSMCs were seeded on cover slips and incubated for 24 h, followed by starvation in serum-free medium for 24 h. The serum-starved cells were pretreated with 20 μM rubiarbonone C for another 24 h. Following stimulation, the cells were treated with 25 ng·mL^{-1} PDGF BB for 24 h and then washed twice in cold PBS. The cells were fixed with cold 4% formaldehyde for 10 min and permeabilized with chilled 0.25% Triton X-100 for 2 min. Then, a blocking step was performed using 3% BSA in PBS for 1 h at room temperature. The cells were incubated with fluorescent phalloidin or primary anti-PCNA or -STAT3 Tyr^{705} antibodies for 1 h, followed by incubation with TRITC- or FITC-labelled secondary antibody for 1 h. Cell nuclei were stained with DAPI, and immunofluorescence images
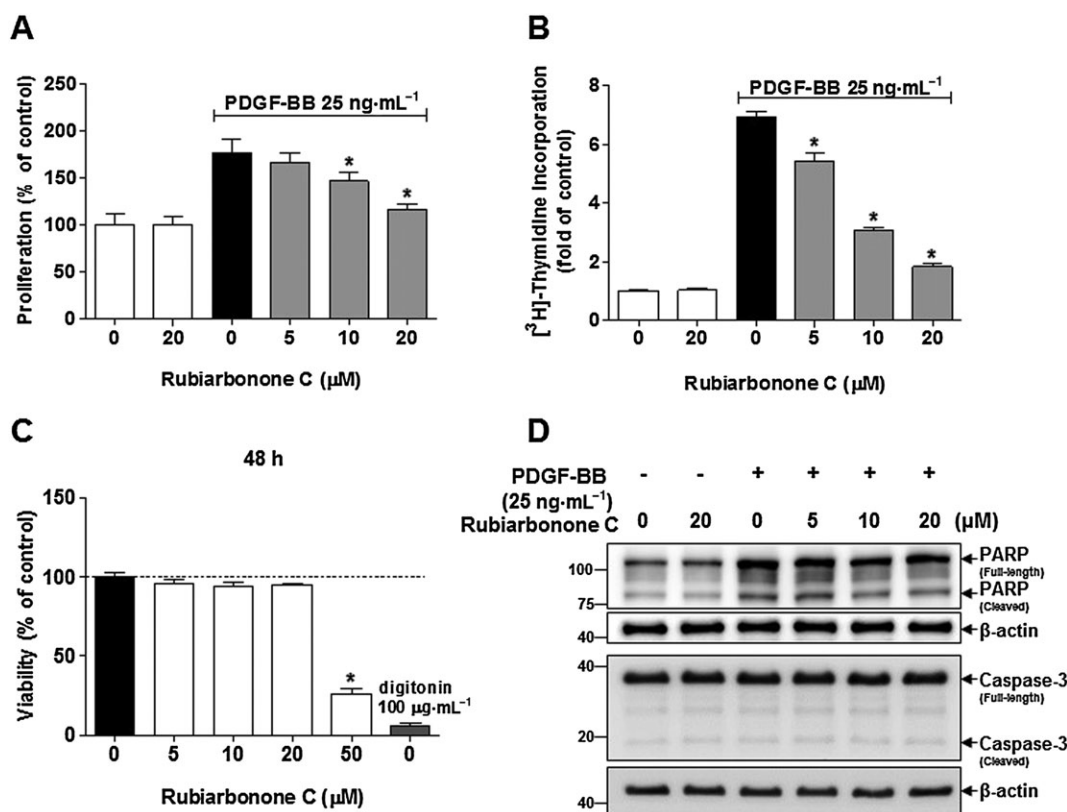

Figure 1

Effects of rubiarbonone C on VSMC proliferation and viability. Serum-starved VSMCs were incubated with rubiarbonone C (5–20 μM) for 24 h followed by 25 ng·mL^{-1} PDGF BB treatment for another 24 h. VSMC proliferation and DNA synthesis were evaluated using the MTT assay (A) and [3H]-thymidine incorporation (B) respectively. (C) VSMCs were cultured in serum-free medium with the control (0.2% DMSO), rubiarbonone C (5–50 μM) or 100 μg·mL^{-1} digitonin (positive control) for 48 h. Cell viability was determined using the MTT assay. Mean values of the control group (untreated group) were set to 100% (A and C) or onefold (B). The values of other groups are presented as % or fold of control values. Means ± SEM (*n* = 5 for each experimental group). *$P < 0.05$ versus PDGF BB alone. (D) VSMC apoptosis was evaluated according to levels of PARP and caspase 3 cleavage (an apoptosis marker). Levels of full-length PARP (116 kDa) and cleaved fragment (89 kDa), and full-length caspase 3 (35 kDa) and cleaved fragment (17–19 kDa) were assessed by Western blotting. The band densities were normalized to those of β-actin signals. The gel images shown are representative of those obtained from three independent experiments.

were obtained using a confocal laser scanning microscope (LSM5 LIVE; Zeiss, Oberkochen, Germany).

Blinding and data normalization

To ensure blinded data analysis, animal surgery was performed by one person, and all images and samples were recorded by another person. Samples extracted from cultured cells and animal experiment were assigned randomly by another person. Data obtained by cell viability assay and Western blot analysis were normalized relative to control (no treatment). The graph Y-axis was labelled as '% of control' or 'fold of control'.

Statistical analyses

The data and statistical analysis comply with the recommendations on experimental design and analysis in pharmacology

(Curtis *et al.*, 2015). All experiments were performed at least three times, and data are expressed as means ± SEM. Statistical analyses were performed using Student's *t*-test or one-way Dunnett's ANOVA, as appropriate (GraphPad ver. 5.01, San Diego, CA, USA). All statistical tests were two-sided, and $P < 0.05$ was considered statistically significant and obtained from five independent experiments.

Materials

Cell culture materials and Alexa Fluor 488 phalloidin were purchased from Invitrogen (Carlsbad, CA, USA). PDGF BB, EGF and TNF-α were obtained from PeproTech (Rocky Hill, NJ, USA). [³H]-thymidine was purchased from AgenBio, Ltd. (Seoul, Korea). MTT, U0126, SP600125, SB203580 and anti-phospho-MARCKS (Ser$^{152/156}$) were from Millipore Corporation (Billerica, MA, USA). Anti-β-actin, anti-cyclin E, anti-cyclin D1,
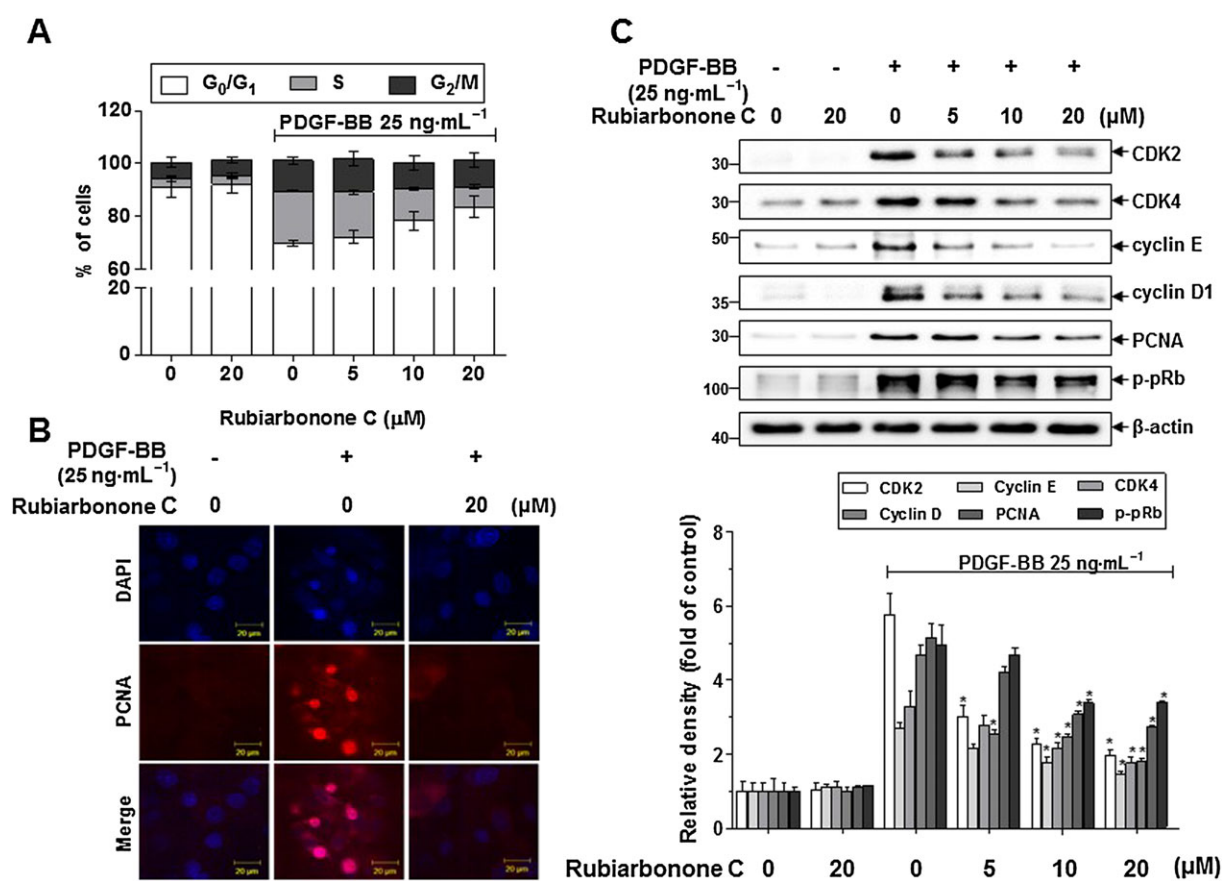

Figure 2

Effects of rubiarbonone C on cell cycle progression and cell cycle regulatory proteins. (A) Effects of rubiarbonone C on cell cycle progression. Serum-deprived VSMCs were incubated with rubiarbonone C (5–20 μM) for 24 h followed by 25 ng·mL^{-1} PDGF BB treatment for 24 h. After DNA staining with PI, the DNA contents of individual nuclei were analysed by flow cytometry. Each value shown was derived from counting >10 000 events. The numbers of cells in the G_0/G_1, S and G_2/M phases are expressed as % of 10 000 events ($n = 3$). (B) PCNA expression was measured by confocal microscopy. After cells were fixed with 4% formaldehyde and membrane-permeabilized using 0.25% Triton X-100, immunofluorescence staining was performed using anti-PCNA and anti-TRITC antibodies. Nuclei were stained with DAPI. Representative immunoblots and immunofluorescence images are shown (scale bar = 20 μm) ($n = 3$). (C) Inhibition by rubiarbonone C of PDGF BB-stimulated expression and activation of cell cycle regulatory proteins. Serum-starved VSMCs were incubated with rubiarbonone C (5–20 μM) for 24 h, followed by 25 ng·mL^{-1} PDGF BB treatment for another 24 h. Levels of CDK2, CDK4, cyclin E, cyclin D1 and PCNA and Rb phosphorylation were determined by Western blotting. The band densities were normalized to those of β-actin signals. Means ± SEM ($n = 5$ for each experimental group). The gel images shown are representative of those obtained from five independent experiments. *$P < 0.05$ versus PDGF BB alone.

anti-CDK2, anti-CDK4, anti-phospho-pRb and anti-PCNA antibodies were obtained from AbFrontier (Geumcheon, Seoul, Korea). Anti-phospho-STAT3 (Tyr[705], Ser[727]), anti-phospho-Src family, anti-ERK1/2, anti-phospho-ERK1/2, anti-p38, anti-phospho-p38, anti-JNK, anti-phospho-JNK, anti-Akt, anti-phospho-Akt, anti-PLCγ1, anti-phospho-PLCγ1, anti-FAK, anti-phospho-FAK (Tyr[397]), anti-phospho-PKC (θ, δ), anti-caspase 3 and anti-MMP2 and anti-MMP9 antibodies were purchased from Cell Signaling Technology, Inc. (Beverly, MA, USA).

Nomenclature of targets and ligands

Key protein targets and ligands in this article are hyperlinked to corresponding entries in http://www.guidetopharmacology.org, the common portal for data from the IUPHAR/BPS Guide to PHARMACOLOGY (Southan *et al.*,

2016), and are permanently archived in the Concise Guide to PHARMACOLOGY 2015/2016 (Alexander *et al.*, 2015a,b).

Results

Effects of rubiarbonone C on PDGF BB-induced VSMC proliferation and viability

To investigate the effect of rubiarbonone C on VSMC function, we measured the vascular activity of rubiarbonone C in PDGF BB-induced VSMC proliferation. Cell proliferation was examined using the MTT assay (Figure 1A) and [3H]-thymidine incorporation (Figure 1B) after cells were pretreated with various concentrations of rubiarbonone C for 24 h, followed by treatment with PDGF BB or 0.2% DMSO as a
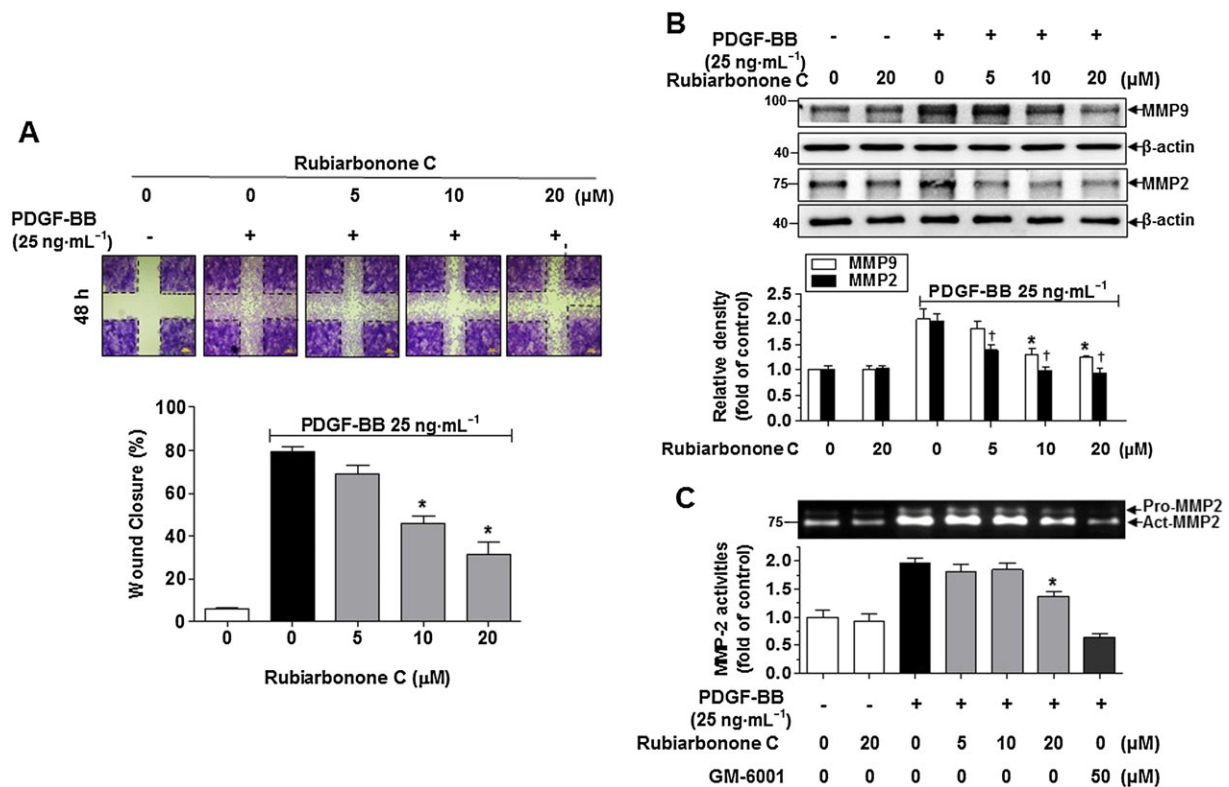

Figure 3

Effects of rubiarbonone C on PDGF-induced VSMC migration. (A) Effects of rubiarbonone C measured using a scratch wound-healing assay. Serum-starved VSMCs were treated with rubiarbonone C (5–20 μM) for 2 h followed by 25 ng·mL^{−1} PDGF BB treatment for 48 h. After 48 h, the cells were stained with 0.5% crystal violet. The images of wound healing are representative of five similar independent experiments, taken at the time of scratching and 48 h after wounding (n = 5 per condition). The dotted line represents a clear zone at time 0 (scale bar = 200 μm). The wound closure area was quantified as % of cells migrating into the wound with respect to the clear area at time 0. The migration area was measured using ImageJ software. (B) Effect of rubiarbonone C on the expression of MMPs. Serum-starved VSMCs were treated with rubiarbonone C (5–20 μM) for 2 h followed by 25 ng·mL^{−1} PDGF BB treatment for 24 h. Cells were lysed and the lysates subjected to Western blotting as described in the Methods section. The band densities were normalized to those of β-actin signals. Means ± SEM (n = 5 for each experimental group). The gel images shown are representative of those obtained from five independent experiments. *P < 0.05 versus PDGF BB alone (MMP9 level), †P < 0.05 versus PDGF BB alone (MMP2 level). (C) Effects of rubiarbonone C on MMP activity. After treatment, conditioned medium was collected and subjected to electrophoresis on a 10% SDS-PAGE gel containing 0.1% gelatin, which was then washed in 2.5% Triton X-100 for 1 h. Band density stained with Coomassie blue R-250 was determined using Quantity One software. The normalization of band densities is described under Methods section. Means ± SEM (n = 5 for each experimental group). *P < 0.05 versus PDGF BB alone.

control (white bar) for another 24 h. As shown in Figure 1A, B, PDGF BB-induced proliferation and [3H]-thymidine incorporation were inhibited significantly by rubiarbonone C in a dose-dependent manner. We also evaluated the anti-proliferative effect of rubiarbonone C on other growth factors using 10% FBS, 50 ng·mL^{-1} EGF and 10 ng·mL^{-1} TNF-α in VSMCs. Rubiarbonone C inhibited cell proliferation induced by the various growth factors as well as PDGF BB, but its inhibitory effect showed the strongest on PDGF BB (Supporting Information Figure S2D). Then, the cytotoxic action of rubiarbonone C was assessed to determine whether the inhibitory effect of rubiarbonone C on VSMC proliferation was due to cytotoxicity or apoptosis (Figure 1C, D). Rubiarbonone C (5–50 μM) had no toxic effects on VSMC after 48 h of exposure (Figure 1C). We also assessed PARP cleavage (from 116 to 89 kDa) and caspase 3 cleavage (from 35 to 17–19 kDa) as apoptosis markers (Soldani and Scovassi, 2002; Son *et al.,* 2016). Although PDGF BB treatment showed an increased level of full length and cleaved forms of PARP, rubiarbonone C treatment did not change PARP expressions. Caspase 3 cleavage also did not show any changes in the PDGF-stimulated VSMC (Figure 1D). It has been known that PARP protein expression is important for a number of cellular functions including expression of inflammatory genes (Espinoza *et al.,* 2007). Since PDGF BB is a mitogen and chemoattractant for VSMC, the increased expression of PARP by PDGF BB seems to be a function related to the regulation of inflammatory genes rather than cell growth. Together, the data indicated that rubiarbonone C regulates PDGF BB-induced VSMC proliferation by blocking DNA synthesis, with no apparent cytotoxicity or apoptosis.

Effect of rubiarbonone C on PDGF BB-mediated cell cycle progression in VSMCs

To examine the mechanism(s) responsible for the anti-proliferative effects of rubiarbonone C, we determined cell cycle progression, using fluorescence-activated cell sorting, and the expression of cell cycle-regulating proteins, using immunofluorescence analyses and Western blotting (Figure 2). When the PDGF BB-stimulated VSMCs were treated with rubiarbonone C, the percentage of cells in S phase decreased in a concentration-dependent manner (Figure 2A). Next, we confirmed the effects on the expression of PCNA, a key protein involved in DNA replication and cell proliferation (Leonardi *et al.,* 1992), using immunofluorescence analysis. Figure 3B shows that the increased expression of PCNA induced by PDGF BB was suppressed significantly by 20 μM rubiarbonone C. We further assessed the protein levels of cell cycle regulatory molecules, and Figure 2C indicates that rubiarbonone C decreased the levels of CDK2, CDK4, cyclin E, cyclin D1 and PCNA and the hyperphosphorylation of pRb in PDGF BB-stimulated VSMCs in a dose-dependent manner. These results suggest that rubiarbonone C suppresses proliferation of VSMCs, with arrest in the G_0/G_1 phase, by inhibiting the expression and activation of cell cycle regulatory proteins.

Effects of rubiarbonone C on PDGF BB-induced VSMC migration via MMP2 and 9

We confirmed the effect of rubiarbonone C on VSMC migration, a major factor in the development and progression of arteriosclerosis and restenosis. To determine the inhibitory
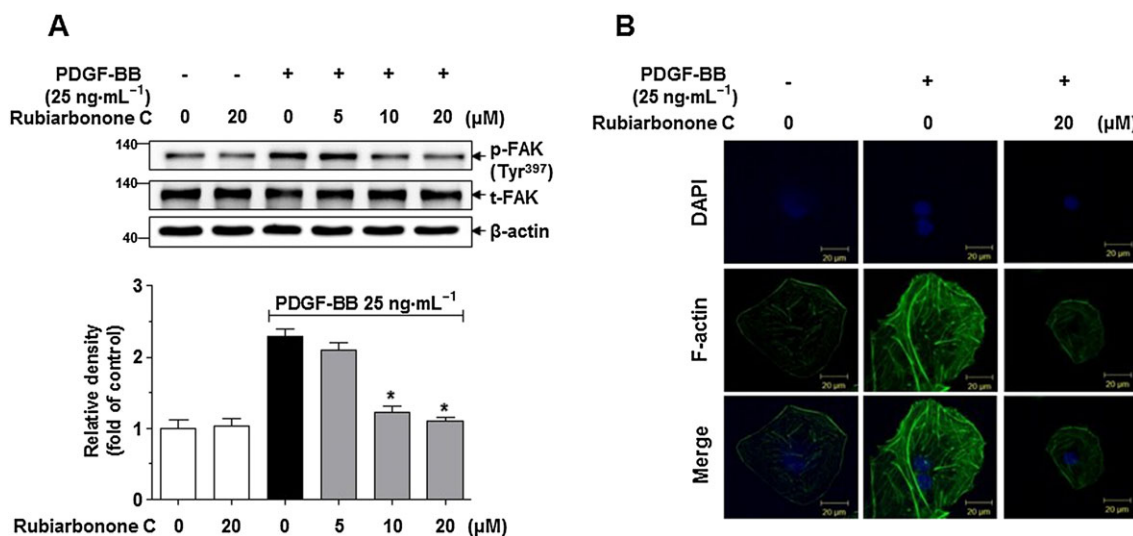

Figure 4

Effects of rubiarbonone C on FAK phosphorylation and F-actin reorganization. (A) Effects of rubiarbonone C on inhibition of PDGF BB-induced FAK Tyr^{397} phosphorylation. Serum-starved VSMCs were incubated with rubiarbonone C (5–20 μM) for 24 h followed by 25 ng·mL^{-1} PDGF BB treatment for 15 min. Phosphor-FAK Tyr^{397} and FAK were assessed by Western blotting. The band densities were normalized to those of total FAK protein expressions. Means ± SEM ($n = 5$ for each experimental group). The gel images shown are representative of those obtained from five independent experiments. *$P < 0.05$ versus PDGF BB alone. Form and density were determined using Quantity One software. (B) Effects of rubiarbonone C on F-actin reorganization in PDGF BB-stimulated VSMCs. Serum-starved VSMCs were incubated with or without 20 μM rubiarbonone C for 24 h, followed by 25 ng·mL^{-1} PDGF BB treatment for another 24 h. F-actin in fixed cells was stained with fluorescent phalloidin for 20 min, and the nuclei were stained with DAPI (scale bar = 20 μm). The F-actin images are representative of three independent experiments ($n = 3$).

action of rubiarbonone C on the migration of VSMCs, serum-starved VSMCs were pretreated with rubiarbonone C for 2 h followed by 25 ng·mL^{-1} PDGF BB treatment. PDGF BB-stimulated VSMC migration was assessed using a wound-healing assay 48 h after inducing the scratches. VSMCs showed an increase wound closure level after PDGF BB stimulation for 48 h, whereas the PDGF BB-induced migration was reduced by 5, 10 and 20 μM rubiarbonone C treatment (Figure 3A). Recently it was reported that TGF-β1 induces MMP-9 expression and this process involves the ROS-dependent ERK-NFκB signalling pathways in VSMCs (Zhang *et al.,* 2013). The antioxidant effect of rubiarbonone C on ROS production was measured using the DPPH and H$_2$DCFDA assay. The H$_2$DCFDA assay is frequently used as a hydrogen peroxide-specific detector in cells and the H$_2$DCFDA has cell-membrane permeability. Intracellular H$_2$DCFDA is changed to DCF by ROS (Oparka *et al.,* 2016). In this experiment, N-acetylcysteine was used for

positive control against antioxidant effect (Kappert *et al.,* 2006). Although rubiarbonone C showed significant antioxidant effect at 200 μM, antioxidant and ROS levels were not effective at 20 μM (Supporting Information Figure S3). However, as shown in Figure 1C, rubiarbonone C has toxic effect on VSMC at 50 μM. Therefore, it suggests that rubiarbonone C has potential antioxidant control capacity but is not effective at the concentrations used in this study. To further evaluate the mechanism of inhibitory action on migration, we assessed the expression and activity of MMP2 and 9, which are involved in VSMC migration through the degradation of extracellular matrix (Li *et al.,* 2015). Figure 3B shows that the expression levels of PDGF BB-stimulated MMP2 and 9 were decreased by rubiarbonone C treatment in a dose-dependent manner. Moreover, according to the gelatin zymographic image (Figure 3C), the activity of MMP2 was inhibited significantly by rubiarbonone C in a dose-dependent manner.
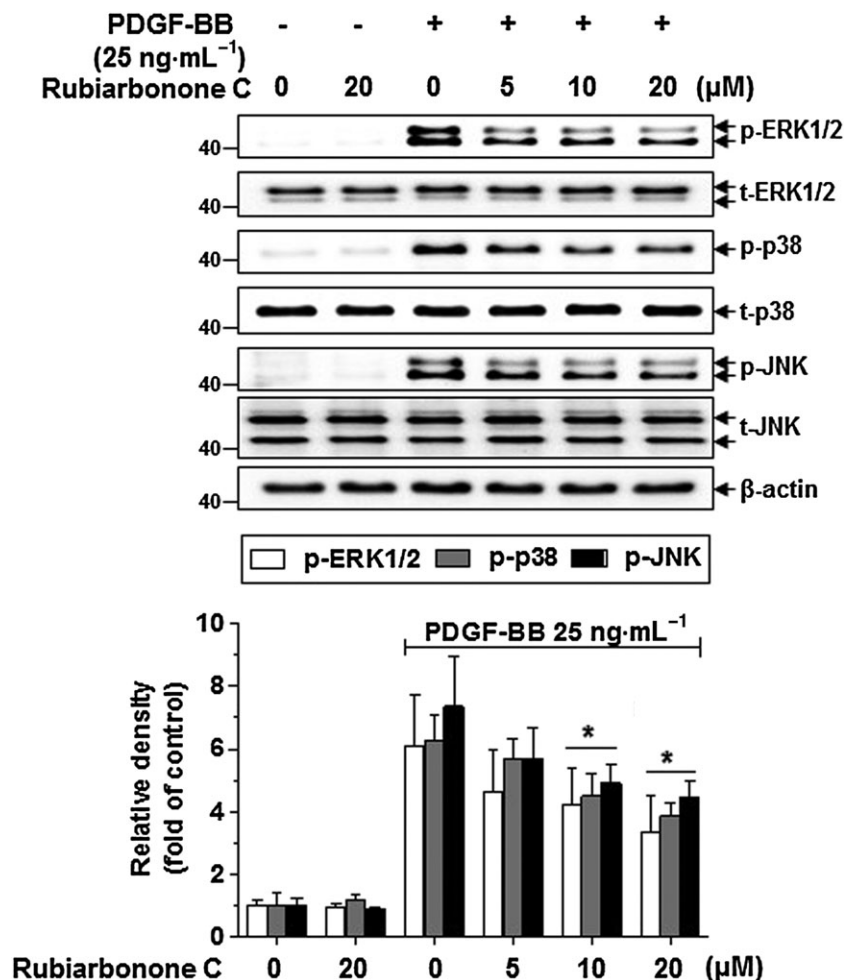

Figure 5

Effects of rubiarbonone C on MAPK components, such as ERK1/2, p38 and JNK. Serum-deprived VSMCs were treated with rubiarbonone C (5–20 μM) for 24 h followed by stimulation with 25 ng·mL^{-1} PDGF BB for 10 min. After stimulation, cells were lysed and the lysates subjected to Western blotting using the antibodies indicated. The bands of phosphorylated proteins were normalized to those of total protein expression. Means ± SEM ($n = 5$ for each experimental group). The gel images shown are representative of those obtained from five independent experiments. *$P < 0.05$ versus PDGF BB alone.

These results indicate that rubiarbonone C inhibited PDGF BB-stimulated VSMC migration *via* decreased MMP2 and 9 levels and MMP2 activity.

Rubiarbonone C regulates PDGF BB-induced VSMC migration via inhibition of FAK activation

To determine whether cytoskeletal reorganization signalling pathways are involved in the effects of rubiarbonone C on VSMC migration, FAK activation and F-actin reorganization were evaluated using Western blotting and immunofluorescence analyses (Figure 4). Quiescent VSMCs were pretreated with various concentrations of rubiarbonone C for 24 h and then stimulated with PDGF BB for 15 min. PDGF BB stimulation strongly induced FAK activation by phosphorylating Tyr[397], whereas 10 and 20 μM rubiarbonone C decreased PDGF BB-induced FAK activation significantly (Figure 4A).

In a separate experiment, cells were fixed and stained with fluorescent phalloidin to observe F-actin by confocal microscopy. PDGF BB-visualized F-actin reorganization was largely abolished by 20 μM rubiarbonone C treatment (Figure 4B). These results demonstrated that rubiarbonone C inhibits VSMC migration *via* inhibition of FAK, resulting in reduced F-actin reorganization in PDGF BB-stimulated VSMCs.

Effects of rubiarbonone C on PDGFR-β signalling in PDGF BB-stimulated VSMCs

To further evaluate whether rubiarbonone C inhibits VSMC proliferation and migration induced by PDGF BB *via* regulating a PDGFR-β downstream signalling pathway, the levels of PLCγ1, PKC, Akt, MAPK and STAT3 were determined by Western blotting and immunofluorescence (Figures 5 and 6; Supporting Information Figure S4). Quiescent VSMCs were pretreated with various concentrations of rubiarbonone C for 24 h followed by PDGF BB treatment for 5 min. Rubiarbonone C showed no apparent effect on the PDGF BB-stimulated activation of PDGFR-β, PLCγ1, Akt, PKC (θ, δ) or MARCKS, the most prominent cellular PKC substrate (Supporting Information Figure S4). However, rubiarbonone C did significantly decrease PDGF BB-induced activation of MAPK proteins, such as ERK1/2, p38 and JNK, in a concentration-dependent manner (Figure 5). When we examined the activation of cytoplasmic protein Src and STAT3 (Tyr[705], Ser[727]), which contribute to PDGF BB-mediated VSMC proliferation and migration (Heiss *et al.*, 2016), PDGF BB strongly induced activation of both Src and STAT3 in VSMCs, whereas rubiarbonone C inhibited the phosphorylation of STAT3 Tyr[705] only and not Src or STAT3 Ser[727] (Figure 6A). To confirm these results, cells were stained by
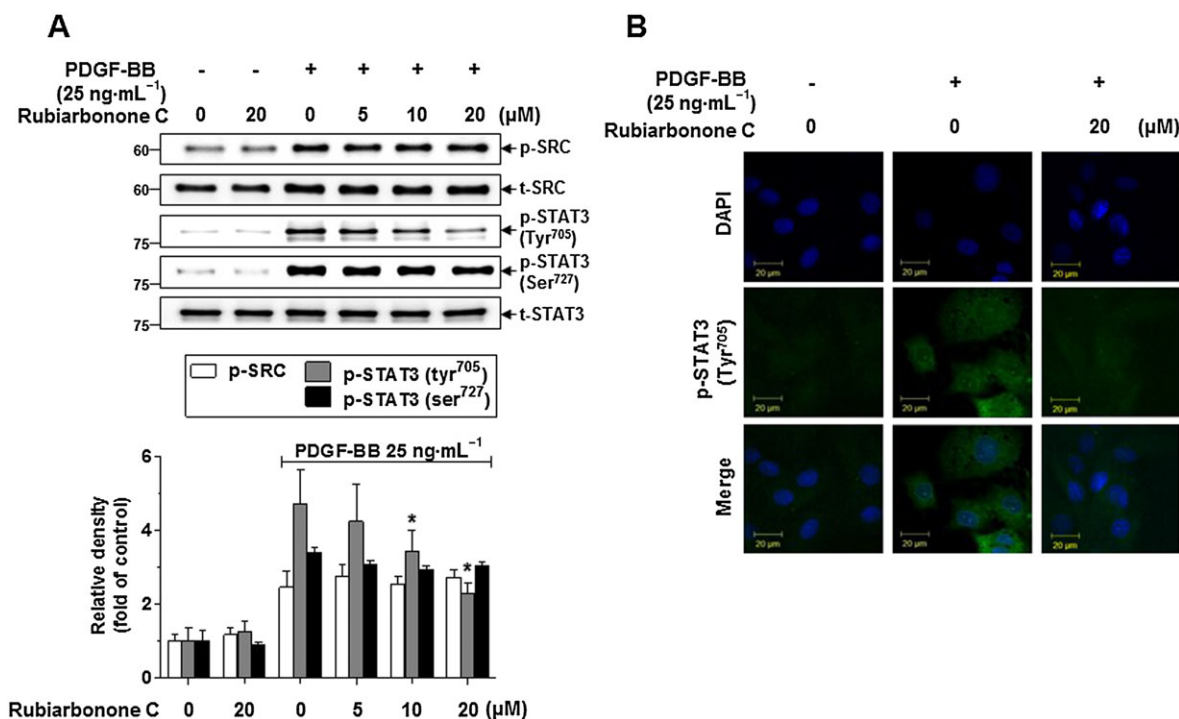

Figure 6

Effects of rubiarbonone C on STAT3 phosphorylation in PDGF BB-stimulated VSMCs (A). Serum-deprived VSMCs were treated with rubiarbonone C (5–20 μM) for 24 h, followed by stimulation with 25 ng·mL^{-1} PDGF BB for 10 min. Cells were lysed and the lysates subjected to Western blotting using the antibodies indicated. The bands of phosphorylated proteins were normalized to those of total protein expression. Means ± SEM ($n = 5$ for each experimental group). The gel images shown are representative of those obtained from five independent experiments. *$P < 0.05$ versus PDGF BB alone. STAT3 Tyr[705] phosphorylation was determined using confocal microscopy (B). Serum-deprived VSMCs were treated with or without 20 μM rubiarbonone C for 24 h, followed by stimulation with PDGF BB for 10 min. Immunofluorescence assays were performed using anti-phospho-STAT3 Tyr[705] and -FITC antibodies and DAPI (scale bar = 20 μm). Images are representative of those obtained from three similar independent experiments ($n = 3$).

immunofluorescence with an anti-STAT3 Tyr[705] antibody and DAPI to visualize the phosphorylation of STAT3 Tyr[705], and the effect of rubiarbonone C on the phosphorylation of STAT3 Tyr[705] was evaluated. Consistent with Figure 6A, phosphorylation of STAT3 Tyr[705] in PDGF BB-stimulated VSMCs was essentially abolished by 20 μM rubiarbonone C (Figure 6B). These results suggest that rubiarbonone C down-regulated activation of the MAPK and STAT3 pathway as PDGFR-β downstream events, inhibiting PDGF BB-induced VSMC proliferation and migration.

Inhibitory effect of rubiarbonone C on STAT3 activation through MAPK regulation in PDGF BB-stimulated VSMCs

To evaluate the effects of rubiarbonone C on STAT3 activation in the MAPK signalling pathway, serum-starved VSMCs were pretreated with 20 μM rubiarbonone C and MAPK inhibitors (U0126 for ERK1/2, SP600125 for JNK, SB203580 for p38) for 2 h followed by treatment with PDGF BB for

10 min. As expected, rubiarbonone C inhibited PDGF BB-activated STAT3 Tyr[705], and this effect was enhanced synergistically by co-treatment with U0126 or SP600125 but not SB203580 (Figure 7A), suggesting involvement of the ERK1/2 and JNK signalling pathways in STAT3 activation. We further assessed whether the MAPK/STAT3 signalling pathway is involved in the inhibitory effect of rubiarbonone C on PDGF BB-induced cell cycle molecules and MMP2 as downstream events. PDGF BB-stimulated phosphorylation of pRb and expression of PCNA were abolished by treatment with rubiarbonone C and by inhibitors of ERK1/2 and JNK but not p38 (Figure 7B, C). However, only ERK1/2 inhibition showed an additive increase in the inhibitory effect of rubiarbonone C on MMP2 expression and activation in PDGF BB-stimulated VSMCs (Figure 7B). When PDGF-induced VSMC proliferation was performed using these inhibitors with rubiarbonone C, inhibition of ERK1/2 and JNK, not p38, inhibited cell proliferation and co-treatment of rubiarbonone C completely inhibited cell proliferation (Figure 7D). Although inhibition of p38 did not involve in
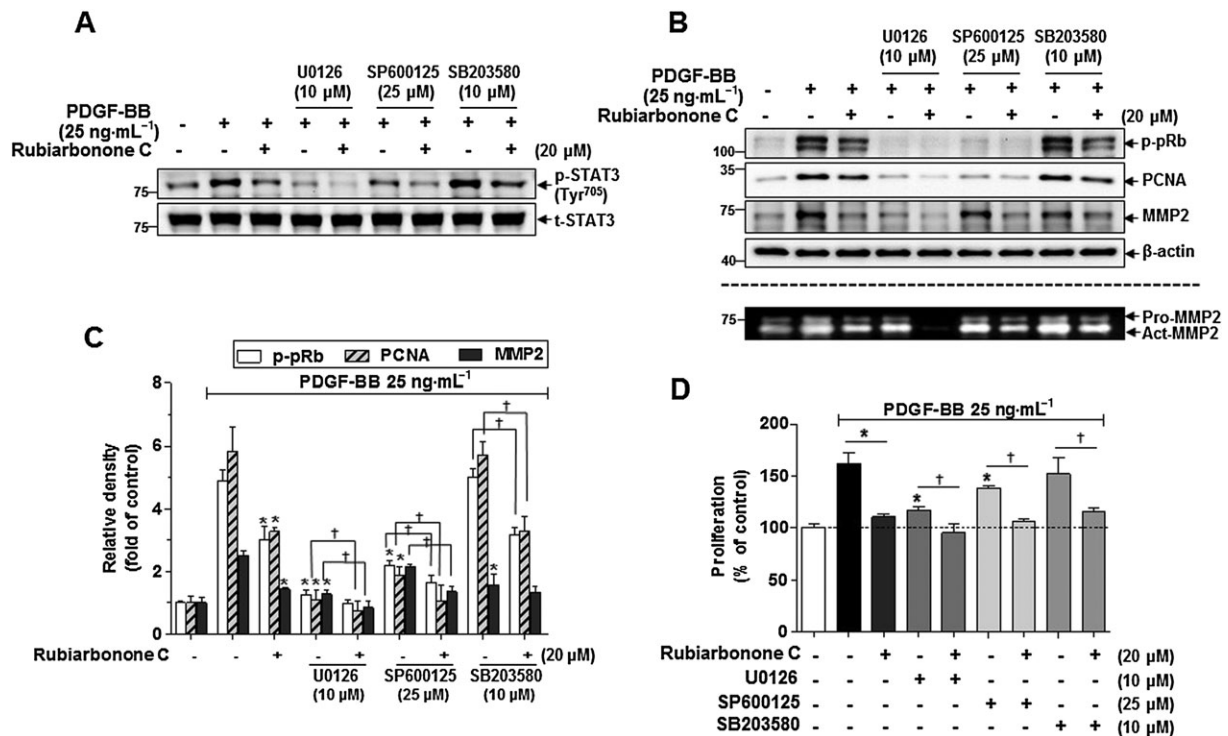

Figure 7

Inhibitory effects of rubiarbonone C on STAT3 Tyr[705] *via* MAPK signalling pathways in PDGF BB-stimulated VSMCs. (A) Inhibition of rubiarbonone C with or without MAPK inhibitors (10 μM U0126 for ERK1/2, 25 μM SP600125 for JNK, 10 μM SB203580 for p38) on the phosphorylation of STAT3 Tyr[705] in PDGF BB-stimulated VSMCs. Serum-starved VSMCs were treated with 20 μM rubiarbonone C along with each MAPK inhibitor for 2 h, followed by 25 ng·mL^{-1} PDGF BB treatment for 10 min. Cells were lysed and the lysates subjected to Western blotting using the antibodies indicated. (B and C) Effect of rubiarbonone C with or without MAPK inhibitors on cell proliferation and migration regulatory proteins in PDGF BB-stimulated VSMCs. For MMP assay, conditioned medium was collected and gelatin zymography assays against MMP2 were performed as described in the Methods section. The band densities were normalized to those of β-actin. Means ± SEM ($n = 5$ for each experimental group). The gel images shown are representative of those obtained from five independent experiments. *$P < 0.05$ versus PDGF BB alone, †$P < 0.05$ versus each inhibitor without rubiarbonone C. (D) Effect of rubiarbonone C in the absence or presence of MAPK inhibitors on cell proliferation levels. VSMCs were pretreated with 20 μM rubiarbonone C along with each MAPK inhibitor for 2 h, followed by PDGF BB treatment for 24 h. VSMC proliferation levels were evaluated by MTT analysis. Means ± SEM ($n = 5$ for each experimental group). *$P < 0.05$ versus PDGF BB alone, †$P < 0.05$ versus each inhibitor without rubiarbonone C.
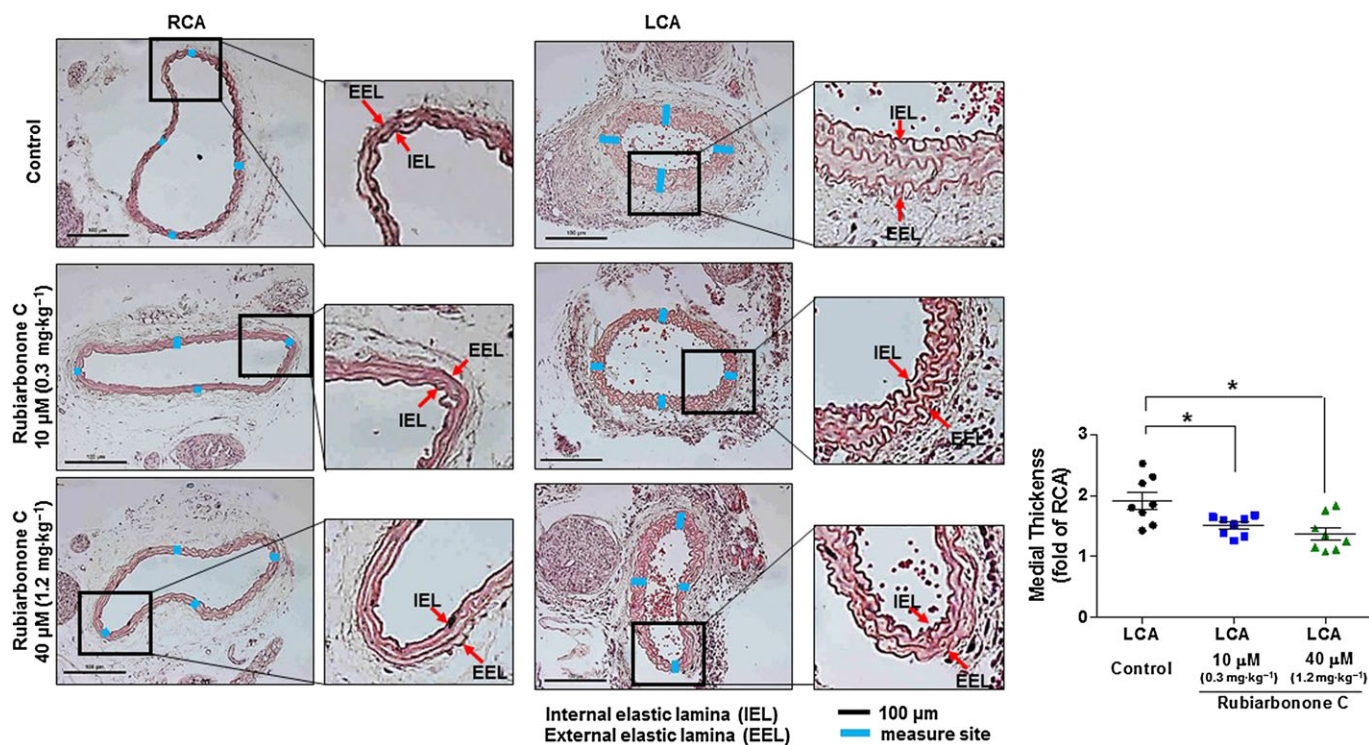
Figure 8

Effect of rubiarbonone C on medial thickness induced by 3 day ligation in mice. C57BL/6 mice in test groups were treated with a low (10 μM, 0.3 mg·kg^{-1}) or high dose (40 μM, 1.2 mg·kg^{-1}) of rubiarbonone C (i.p.) for 3 days. After 24 h of the first injection, the LCA of the mouse was ligated. After 3 days of ligation, carotid arteries were harvested, fixed and embedded in paraffin. The medial thickness of the ligated LCA was measured and compared to that of unligated right carotid artery (RCA). Representative light microscopy images of haematoxylin and eosin-stained carotid artery cross sections were from control (LCA ligated, but no rubiarbonone C treatment) and the rubiarbonone C treated-mice. Means ± SEM ($n = 8$ for each experimental group). The images shown are representative of those obtained from eight independent experiments. *$P < 0.05$ versus LCA control.
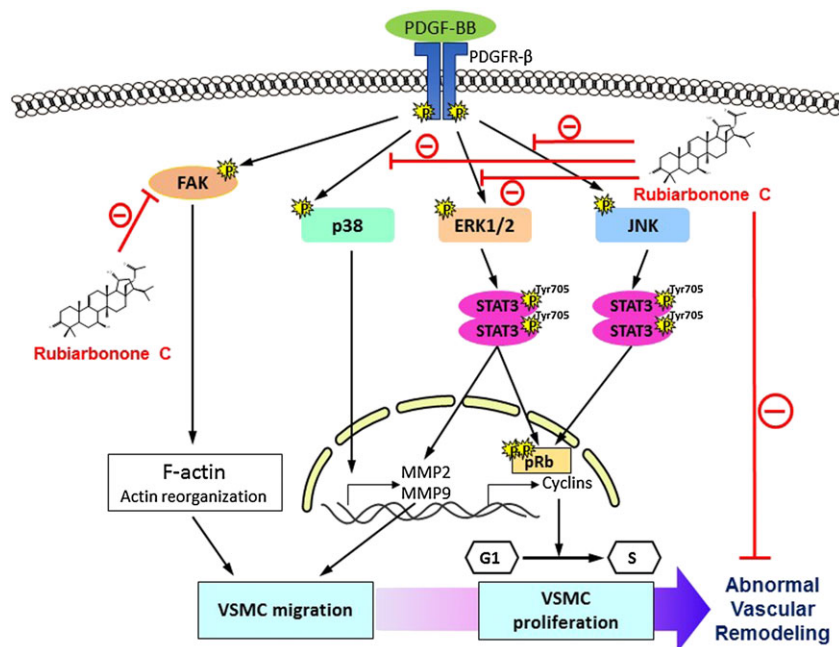

Figure 9

Proposed scheme for the inhibitory effects of rubiarbonone C on the proliferation and migration of PDGF BB-stimulated VSMCs.

cell proliferation, co-treatment with rubiarbonone C significantly inhibited cell proliferation. These inhibitory effects of cell proliferation are due to the inhibition of ERK1/2 and JNK by rubiarbonone. Together, these results suggest that the inhibitory effect of rubiarbonone C on PDGF-induced proliferation occurred *via* regulation of ERK1/2- and JNK-mediated STAT3 activation, and the inhibitory effect on migration occurred *via* regulation of ERK1/2-mediated STAT3-MMP2 activation.

Effect of rubiarbonone C on medial thickness after carotid ligation

It has been reported that ligation of carotid artery induces shear stress and inflammation, which increases cytokine and growth factor secretion, and subsequently stimulates the activation of VSMCs. The activated VSMCs increase medial thickness and neointimal formation through migration and proliferation (McPherson *et al.,* 2001; Heo *et al.,* 2014a,b). Thus, mouse carotid artery ligation is an excellent animal model for evaluating the atherosclerosis development caused by VSMC proliferation and migration. To determine the effect of rubiarbonone C on the suppression of ligation-induced medial thickness, the area of media in blood vessels was measured using mouse carotid ligation model. The medial thickness was induced by LCA ligation for 3 days (Figure 8). The treatment with rubiarbonone C 10 and 40 μM significantly diminished ligation-induced medial thickness by 44.96 and 59.3% respectively. The organ toxicity of rubiarbonone C was confirmed by performing histology and Western blot for checking the cleavage of PARP and caspase 3 in various organs including heart, lungs, liver, spleen and kidney. The tissues from rubiarbonone-C-injected groups did not show any either histological change or cleaved form of PARP and caspase-3 as compared to control (no rubiarbonone C treatment), and the body weights of mice were not significantly changed during the experiment period (Supporting Information Figure S5).

Discussion and conclusions

We demonstrated that rubiarbonone C inhibited PDGF BB-induced proliferation and migration of VSMCs potently. Indeed, our study yielded three major findings. First, rubiarbonone C caused G_0/G_1 cell cycle arrest and inhibition of MMP2 and 9 in PDGF BB-stimulated VSMCs. Second, the signalling molecules targeted by rubiarbonone C for the regulation of PDGF-stimulated VSMC proliferation and migration were MAPK and FAK. Third, rubiarbonone C regulated ERK1/2- and JNK-mediated STAT3 activation, resulting in inhibition of cell cycle progression of VSMCs, and it inhibited ERK1/2-mediated STAT3 activation, resulting in suppressed expression and activity of MMP2 in VSMC migration. Rubiarbonone C also inhibited FAK directly, blocking F-actin reorganization. These events are illustrated in Figure 9.

A key mechanism for inhibiting cell proliferation is the regulation of cell cycle components (Braun-Dullaeus *et al.,* 2004). Indeed, rubiarbonone C significantly inhibited PDGF BB-induced protein levels of CDK2, CDK4, cyclin E and cyclin D1, which normally regulate progression of the cell cycle from

the G_0/G_1 to S phase (Figures 1C, D and 2). Additionally, PCNA expression and pRb phosphorylation were down-regulated by rubiarbonone C in PDGF BB-stimulated VSMCs, suggesting an important role for rubiarbonone C in regulating cell cycle progression to S phase. Increased CDK inhibitors, such as p21 and p27, have been demonstrated to inhibit checkpoint proteins in the cell cycle (Donovan and Slingerland, 2000). Thus, it seems possible that rubiarbonone C suppresses PDGF BB-induced increases in the expression of cell cycle checkpoint proteins by up-regulating CDK inhibitors.

We also confirmed that rubiarbonone C inhibited PDGF BB-induced VSMC migration *via* down-regulation of both the expression and activity of MMP2 and 9 (Figure 3). Thus, rubiarbonone C may inhibit cell migration by inhibiting external substrate degradation mediated by MMP2 and 9 (Remacle *et al.,* 2011). The activation of FAK has also been suggested to play an important role in the reorganization of the cytoskeleton for cell movement (Wu *et al.,* 2015). Consistent with a previous report, rubiarbonone C suppressed FAK activation and F-actin reorganization significantly (Figure 4).

Because PDGFR-β activation by PDGF BB is a key process involved in dysregulation of VSMC proliferation and migration (Cagnin *et al.,* 2009), we further evaluated the effect of rubiarbonone C on the activation of PDGFR-β and its downstream signalling molecules, including PLCγ, PKC, MARCKS and Akt, as reported previously (Yu *et al.,* 2015). Although PDGF BB strongly activated these signalling molecules, as well as PDGFR-β, their activation was not inhibited by rubiarbonone C (Supporting Information-Figure S4). This showed that the inhibitory effect of rubiarbonone C on VSMC proliferation and migration did not involve PDGFR-β-mediated signalling pathways. Instead, our data indicated that the activation of MAPK family members, such as ERK1/2, JNK and p38, was largely significantly abolished by rubiarbonone C in PDGF BB-stimulated VSMCs (Figure 5).

Phosphorylation of STAT3 Tyr[705] was decreased significantly by rubiarbonone C in PDGF BB-stimulated VSMCs, whereas rubiarbonone C had no apparent effect on the phosphorylation of STAT3 Ser[727] or Src activation, a molecule upstream of STAT3 (Figure 6A). It has been suggested that phosphorylation of STAT3 Tyr[705] induces formation of STAT3 dimers and their translocation into the nucleus, where STAT3 acts as a transcription factor (Takeda *et al.,* 1997). We showed that rubiarbonone C significantly inhibited STAT3 dimers induced by Tyr[705] phosphorylation in a dose-dependent manner and subsequent STAT3 activation in the cytoplasm and nucleus (Figure 6). Unlike the effects of the tyrosine kinase inhibitor BMS-354825 on the tyrosine activities of PDGF receptor/Src/STAT3 (Chen *et al.,* 2006), rubiarbonone C only inhibited activation of STAT3. Additionally, rubiarbonone C inhibited a PDGF BB-stimulated MAPK signalling pathway, and this pathway was involved differently in STAT3 activation in regulating VSMC proliferation and migration (Figure 7). These results suggest that inhibition of only one MAPK family member is not sufficient to regulate abnormal VSMC function, and rubiarbonone C selectively inhibits MAPK family members. A recent report showed that down-regulation of STAT3 resulted in inhibition

of cyclin D1 and MMP9 expression and inactivation of pRb in VSMC proliferation and migration (Park *et al.,* 2015). In our study, phosphorylation of STAT3 Tyr[705] was mediated by ERK1/2 and JNK, and treatment with rubiarbonone C and U0126 inhibited the activation of STAT3 synergistically, as well as Rb phosphorylation and PCNA expression, in PDGF BB-stimulated VSMCs. Additionally, rubiarbonone C inhibited MMP2 *via* regulation of ERK1/2-mediated STAT3 activation (Figure 7). We also confirmed that the ligation-induced medial thickness of carotid artery in mouse was significantly diminished by rubiarbonone C without any toxicity (Figure 8; Supporting Information Figure S5A, B). These results indicated that rubiarbonone C inhibition of ERK1/2 and JNK cooperatively inhibited STAT3 activation, affecting the levels of proteins regulating proliferation and migration.

In conclusion, our study showed that rubiarbonone C from *R. philippinensis* inhibits the ERK1/2, JNK and p38 signalling pathways, rather than the PDGFR-β-mediated tyrosine kinase pathway, and that these signalling pathways differentially control STAT3 activation, leading to PDGF BB-induced cell proliferation and migration. VSMC proliferation and migration are key events in the development of vascular restenosis associated with angioplasty and stenting procedures for coronary artery diseases. Our study provides the first reported evidence that rubiarbonone C has the potential to modulate VSMC proliferation and migration through inhibition of PDGF-mediated signalling pathway, suggesting that rubiarbonone C could be a good candidate for the treatment of cardiovascular disease.

Acknowledgements

Author contributions

H.S.P., K.S.H. and C.S.M. designed the study, analysed the data and wrote the manuscript. H.S.P., J.H.H., S.H.J., D.H.L., E.J. and T.W.L. performed the experiments and analysed the data. K.T.Q. and M.N. helped with the rubiarbonone C preparation and data analysis.

Conflict of interest

The authors declare no conflicts of interest.

Declaration of transparency and scientific rigour

This Declaration acknowledges that this paper adheres to the principles for transparent reporting and scientific rigour of preclinical research recommended by funding agencies, publishers and other organisations engaged with supporting research.

References

Alexander SPH, Fabbro D, Kelly E, Marrion N, Peters JA, Benson HE *et al.* (2015a). The Concise Guide to PHARMACOLOGY 2015/16: Catalytic receptors. Br J Pharmacol 172: 5979–6023.

Alexander SPH, Fabbro D, Kelly E, Marrion N, Peters JA, Benson HE *et al.* (2015b). The Concise Guide to PHARMACOLOGY 2015/16: Enzymes. Br J Pharmacol 172: 6024–6109.

Amoussa AM, Lagnika L, Bourjot M, Vonthron-Senecheau C, Sanni A (2016). Triterpenoids from Acacia ataxacantha DC: antimicrobial and antioxidant activities. BMC Complement Altern Med 16: 284.

Bicknell KA, Surry EL, Brooks G (2003). Targeting the cell cycle machinery for the treatment of cardiovascular disease. J Pharm Pharmacol 55: 571–591.

Braun-Dullaeus RC, Mann MJ, Sedding DG, Sherwood SW, von der Leyen HE, Dzau VJ (2004). Cell cycle-dependent regulation of smooth muscle cell activation. Arterioscler Thromb Vasc Biol 24: 845–850.

Cagnin S, Biscuola M, Patuzzo C, Trabetti E, Pasquali A, Laveder P *et al.* (2009). Reconstruction and functional analysis of altered molecular pathways in human atherosclerotic arteries. BMC Genomics 10: 13.

Chaabane C, Otsuka F, Virmani R, Bochaton-Piallat ML (2013). Biological responses in stented arteries. Cardiovasc Res 99: 353–363.

Chan KC, Ho HH, Lin MC, Yen CH, Huang CN, Huang HP *et al.* (2014). Mulberry water extracts inhibit atherosclerosis through suppression of the integrin-β₃/focal adhesion kinase complex and downregulation of nuclear factor κB signaling *in vivo* and *in vitro*. J Agric Food Chem 62: 9463–9471.

Chandra A, Angle N (2006). VEGF inhibits PDGF-stimulated calcium signaling independent of phospholipase C and protein kinase C. J Surg Res 131: 302–309.

Chen WQLX, Gao YZ, Ruan YZ (1999). Rubiaceae. In: Flora of China, Zhengyi Wu, Peter Raven: St. Louis. Vol. 19, pp. 287–318.

Chen Z, Lee FY, Bhalla KN, Wu J (2006). Potent inhibition of platelet-derived growth factor-induced responses in vascular smooth muscle cells by BMS-354825 (dasatinib). Mol Pharmacol 69: 1527–1533.

Chistiakov DA, Orekhov AN, Bobryshev YV (2015). Vascular smooth muscle cell in atherosclerosis. Acta Physiol (Oxf) 214: 33–50.

Curtis MJ, Bond RA, Spina D, Ahluwalia A, Alexander SP, Giembycz MA *et al.* (2015). Experimental design and analysis and their reporting: new guidance for publication in BJP. Br J Pharmacol 172: 3461–3471.

Donovan J, Slingerland J (2000). Transforming growth factor-β and breast cancer: cell cycle arrest by transforming growth factor-β and its disruption in cancer. Breast Cancer Res 2: 116–124.

Elmer ADE (1934). Leaflets of Philippine Botany. Manila. In: Elmer ADE (ed). New uticaceae and rubiaceae. A.M.: Manial, p. 3214.

Espinoza LA, Smulson ME, Chen Z (2007). Prolonged poly(ADP-ribose) polymerase-1 activity regulates JP-8-induced sustained cytokine expression in alveolar macrophages. Free Radic Biol Med 42: 1430–1440.

Fan JT, Kuang B, Zeng GZ, Zhao SM, Ji CJ, Zhang YM *et al.* (2011). Biologically active arborinane-type triterpenoids and anthraquinones from *Rubia yunnanensis*. J Nat Prod 74: 2069–2080.

Fredriksson L, Li H, Eriksson U (2004). The PDGF family: four gene products form five dimeric isoforms. Cytokine Growth Factor Rev 15: 197–204.

Gao Y, Su Y, Huo Y, Mi J, Wang X, Wang Z *et al*. (2014). Identification of antihyperlipidemic constituents from the roots of *Rubia yunnanensis* Diels. J Ethnopharmacol 155: 1315–1321.

Garcia-Rivas G, Youker KA, Orrego C, Flores-Arredondo J, Guerrero-Beltran CE, Cordero-Reyes A *et al*. (2015). Standardized extracts from black bean coats (*Phaseolus vulgaris* L.) prevent adverse cardiac remodeling in a murine model of non-ischemic cardiomyopathy. RSC Adv 5: 90858–90865.

Han JH, Lee SG, Jung SH, Lee JJ, Park HS, Kim YH *et al*. (2015). Sesamin inhibits PDGF-mediated proliferation of vascular smooth muscle cells by upregulating p21 and p27. J Agric Food Chem 63: 7317–7325.

Heiss EH, Schachner D, Donati M, Grojer CS, Dirsch VM (2016). Increased aerobic glycolysis is important for the motility of activated VSMC and inhibited by indirubin-3′-monoxime. Vascul Pharmacol 83: 47–56.

Heo KS, Cushman HJ, Akaike M, Woo CH, Wang X, Qiu X *et al*. (2014a). ERK5 activation in macrophages promotes efferocytosis and inhibits atherosclerosis. Circulation 130: 180–191.

Heo KS, Fujiwara K, Abe J (2014b). Shear stress and atherosclerosis. Mol Cells 37: 435–440.

Hu C, Liu S, Sun Y, Shi G, Li Y (2014). Effect of recombinant hPTEN gene expression on PDGF induced VSMC proliferation. Cell Biochem Biophys 70: 1185–1190.

Jun MY, Karki R, Paudel KR, Sharma BR, Adhikari D, Kim DW (2016). Alkaloid rich fraction from *Nelumbo nucifera* targets VSMC proliferation and migration to suppress restenosis in balloon-injured rat carotid artery. Atherosclerosis 248: 179–189.

Kang H, Ahn DH, Pak JH, Seo KH, Baek NI, Jang SW (2016). Magnobovatol inhibits smooth muscle cell migration by suppressing PDGF-Rβ phosphorylation and inhibiting matrix metalloproteinase-2 expression. Int J Mol Med 37: 1239–1246.

Kappert K, Sparwel J, Sandin A, Seiler A, Siebolts U, Leppanen O *et al*. (2006). Antioxidants relieve phosphatase inhibition and reduce PDGF signaling in cultured VSMCs and in restenosis. Arterioscler Thromb Vasc Biol 26: 2644–2651.

Kilkenny C, Browne W, Cuthill IC, Emerson M, Altman DG (2010). Animal research: reporting *in vivo* experiments: the ARRIVE guidelines. Br J Pharmacol 160: 1577–1579.

Kim J, Ko J (2014). Human sLZIP promotes atherosclerosis via MMP-9 transcription and vascular smooth muscle cell migration. FASEB J 28: 5010–5021.

Kim JH, Jin YR, Park BS, Kim TJ, Kim SY, Lim Y *et al*. (2005). Luteolin prevents PDGF BB-induced proliferation of vascular smooth muscle cells by inhibition of PDGFβ-receptor phosphorylation. Biochem Pharmacol 69: 1715–1721.

Kuok QY, Yeh CY, Su BC, Hsu PL, Ni H, Liu MY *et al*. (2013). The triterpenoids of Ganoderma tsugae prevent stress-induced myocardial injury in mice. Mol Nutr Food Res 57: 1892–1896.

Kupai K, Szucs G, Cseh S, Hajdu I, Csonka C, Csont T *et al*. (2010). Matrix metalloproteinase activity assays: importance of zymography. J Pharmacol Toxicol Methods 61: 205–209.

Lajko E, Banyai P, Zambo Z, Kursinszki L, Szoke E, Kohidai L (2015). Targeted tumor therapy by *Rubia tinctorum* L.: analytical characterization of hydroxyanthraquinones and investigation of their selective cytotoxic, adhesion and migration modulator effects

on melanoma cell lines (A2058 and HT168-M1). Cancer Cell Int 15: 119.

Lee JE, Hitotsuyanagi Y, Fukaya H, Kondo K, Takeya K (2008). New cytotoxic bicyclic hexapeptides, RA-XXIII and RA-XXIV, from *Rubia cordifolia* L. Chem Pharm Bull(Tokyo) 56: 730–733.

Lee JJ, Yu JY, Zhang WY, Kim TJ, Lim Y, Kwon JS *et al*. (2011a). Inhibitory effect of fenofibrate on neointima hyperplasia via G_0/G_1 arrest of cell proliferation. Eur J Pharmacol 650: 342–349.

Lee JJ, Zhang WY, Yi H, Kim Y, Kim IS, Shen GN *et al*. (2011b). Anti-proliferative actions of 2-decylamino-5,8-dimethoxy-1,4-naphthoquinone in vascular smooth muscle cells. Biochem Biophys Res Commun 411: 213–218.

Leonardi E, Girlando S, Serio G, Mauri FA, Perrone G, Scampini S *et al*. (1992). PCNA and Ki67 expression in breast carcinoma: correlations with clinical and biological variables. J Clin Pathol 45: 416–419.

Li PC, Sheu MJ, Ma WF, Pan CH, Sheu JH, Wu CH (2015). Anti-restenotic roles of dihydroaustrasulfone alcohol involved in inhibiting PDGF-BB-stimulated proliferation and migration of vascular smooth muscle cells. Mar Drugs 13: 3046–3060.

Liou MJ, Wu TS (2002). Triterpenoids from *Rubia yunnanensis*. J Nat Prod 65: 1283–1287.

Lodi S, Sharma V, Kansal L (2011). The protective effect of *Rubia cordifolia* against lead nitrate-induced immune response impairment and kidney oxidative damage. Indian J Pharmcol 43: 441–444.

McGrath JC, Lilley E (2015). Implementing guidelines on reporting research using animals (ARRIVE etc.): new requirements for publication in BJP. Br J Pharmacol 172: 3189–3193.

McPherson JA, Barringhaus KG, Bishop GG, Sanders JM, Rieger JM, Hesselbacher SE *et al*. (2001). Adenosine A_{2A} receptor stimulation reduces inflammation and neointimal growth in a murine carotid lgation model. Arterioscler Thromb Vasc Biol 21: 791–796.

Muhammad D, Hubert J, Lalun N, Renault JH, Bobichon H, Nour M *et al*. (2015). Isolation of flavonoids and triterpenoids from the fruits of *Alphitonia neocaledonica* and evaluation of their anti-oxidant, anti-tyrosinase and cytotoxic activities. Phytochem Anal 26: 137–144.

Oparka M, Walczak J, Malinska D, van Oppen LM, Szczepanowska J, Koopman WJ *et al*. (2016). Quantifying ROS levels using CM-H_2DCFDA and HyPer. Methods 109: 3–11.

Park S, Kim JK, Oh CJ, Choi SH, Jeon JH, Lee IK (2015). Scoparone interferes with STAT3-induced proliferation of vascular smooth muscle cells. Exp Mol Med 47: e145.

Remacle AG, Shiryaev SA, Radichev IA, Rozanov DV, Stec B, Strongin AY (2011). Dynamic interdomain interactions contribute to the inhibition of matrix metalloproteinases by tissue inhibitors of metalloproteinases. J Biol Chem 286: 21002–21012.

Sachinidis A, Flesch M, Ko Y, Schror K, Bohm M, Dusing R *et al*. (1995). Thromboxane A_2 and vascular smooth muscle cell proliferation. Hypertension 26: 771–780.

da Silva PL, do Amaral VC, Gabrielli V, Montt Guevara MM, Mannella P, Baracat EC *et al*. (2015). Prolactin promotes breast cancer cell migration through actin cytoskeleton remodeling. Front Endocrinol (Lausanne) 6: 186.

Soldani C, Scovassi AI (2002). Poly(ADP-ribose) polymerase-1 cleavage during apoptosis: an update. Apoptosis 7: 321–328.

Son DJ, Jung JC, Hong JT (2016). Epothilones suppress neointimal thickening in the rat carotid balloon-injury model by inducing vascular smooth muscle cell apoptosis through p53-dependent signaling pathway. PLoS One 11: e0155859.

Southan C, Sharman JL, Benson HE, Faccenda E, Pawson AJ, Alexander SPH et al. (2016). The IUPHAR/BPS guide to PHARMACOLOGY in 2016: towards curated quantitative interactions between 1300 protein targets and 6000 ligands. Nucl Acids Res 44: D1054–D1068.

Takeda K, Noguchi K, Shi W, Tanaka T, Matsumoto M, Yoshida N et al. (1997). Targeted disruption of the mouse Stat3 gene leads to early embryonic lethality. Proc Natl Acad Sci U S A 94: 3801–3804.

Wu L, Wang X, Liu Q, Wingnang Leung A, Wang P, Xu C (2015). Sinoporphyrin sodium mediated photodynamic therapy inhibits the migration associated with collapse of F-actin filaments cytoskeleton in MDA-MB-231 cells. Photodiagnosis Photodyn Ther 13: 58–65.

Yin K, Agrawal DK (2014). High-density lipoprotein: a novel target for antirestenosis therapy. Clin Transl Sci 7: 500–511.

Yu D, Makkar G, Strickland DK, Blanpied TA, Stumpo DJ, Blackshear PJ et al. (2015). Myristoylated alanine-rich protein kinase substrate (MARCKS) regulates small GTPase Rac1 and Cdc42 activity and is a critical mediator of vascular smooth muscle cell migration in intimal hyperplasia formation. J Am Heart Assoc 4: e002255.

Zhang H, Wang ZW, Wu HB, Li Z, Li LC, Hu XP et al. (2013). Transforming growth factor-beta1 induces matrix metalloproteinase-9 expression in rat vascular smooth muscle cells via ROS-dependent ERK-NF-κB pathways. Mol Cell Biochem 375: 11–21.

Supporting Information

Additional Supporting Information may be found online in the supporting information tab for this article.

https://doi.org/10.1111/bph.13986

Figure S1 Structure of rubiarbonone C.

Figure S2 Inhibitory effect of rubiarbonone C on various growth factors induced-VSMCs proliferation. (A) VSMCs were cultured in 96-well plates and applied serum starvation for 24 h. The cells were treated with 20 μM rubiarbonone C for 24 h followed by treatment with the indicated concentrations of PDGF BB for another 24 h. (B) Line graph indicates the inhibitory effect of rubiarbonone C (20 μM) on various concentrations (5 to 100 ng/mL) of PDGF BB-induced cell proliferation (△proliferation (%) = PDGF BB treatment only – PDGF BB with 20 μM rubiarbonone C treatment). (C) Inhibition level of VSMCs growth on various dose of rubiarbonone C. (D) Serum-starved VSMCs were pretreated 20 μM rubiarbonone C for 24 h. The VSMCs were then stimulated with the 25 ng·mL^{-1} PDGF BB, 10% FBS, 50 ng·mL^{-1} EGF, or 10 ng·mL^{-1} TNF-α for another 24 h. VSMCs proliferation levels were measured using a MTT assay. Statistical differences from the indicated-control are demonstrated by *$P < 0.05$.

Figure S3 Effects of rubiarbonone C on antioxidant and ROS level. (A) The DPPH free radical scavenging activity of rubiarbonone C (20 or 200 μM) or NAC (20–2000 μM) (positive control) were measured as described in Methods. Statistical differences from the control (nothing treated) are indicated by *$P < 0.05$. (B) Effects of rubiarbonone C on the production of ROS in PDGF BB-stimulated VSMCs. VSMCs were pretreated with rubiarbonone C (5–20 μM) or 2 mM NAC for 24 h, and then incubated with 25 ng·mL^{-1} PDGF BB for 1 h. After stimulation, the cells were stained by 20 μM H2DCFDA for 30 min at 37°C. Statistical differences from the PDGF BB control (PDGF BB stimulated, but no rubiarbonone C) are indicated by *$P < 0.05$.

Figure S4 Effects of rubiarbonone C on PDGFR-β downstream signalling pathway components, including PDGFR-β, PLCγ1, PKC(θ/δ), MARCKS, and Akt. Serum-deprived VSMCs were treated with rubiarbonone C (5–20 μM) for 24 h followed by stimulation with 25 ng·mL^{-1} PDGF BB for various times (3–15 min). After stimulation, cells were lysed and the lysates subjected to Western blotting using the antibodies indicated. Bands were normalized to those of β-actin or total protein.

Figure S5 Effect of rubiarbonone C on organ toxicity. (A) Histological images of liver, spleen, kidney, heart and lung (H&E statin, scale bar = 100 μm). (B) Gel images of the expression of apoptosis markers, the cleavage of PARP cleavage and caspase-3 in liver, spleen, kidney, heart and lung. Bands were normalized to those of β-actin. (C) The changes of body weight in during experimental period using mouse carotid ligation model.